Journal of Energy Storage 132 (2025) 117840

Contents lists available at ScienceDirect

Journal of Energy Storage

journal homepage: www.elsevier.com/locate/est

Research Papers

An optimization cost strategy for storage-enabled hydrogen flow network using Monte Carlo simulation

M.B. Rasheed *, Daniel Rodriguez, Maria D. R-Moreno

Universidad de Alcalá, Escuela Politécnica Superior, Alcalá de Henares, 28805, Madrid, Spain

ARTICLE INFO

Keywords:
Hydrogen gas network
Storage unit
Monte Carlo simulation
Graph theory
Optimization strategy

ABSTRACT

This article presents an innovative approach to address the optimization and planning of hydrogen network transmission, focusing on minimizing computational and operational costs, including capital, operational, and maintenance expenses. The mathematical models developed for gas flow rate, pipelines, junctions, and storage form the basis for the optimization problem, which aims to reduce costs while satisfying equality, inequality, and binary constraints. To achieve this, we implement a dynamic algorithm incorporating 100 scenarios to account for uncertainty. Unlike conventional successive linear programming methods, our approach solves successive piecewise problems and allows comparisons with other techniques, including stochastic and deterministic methods. Our method significantly reduces computational time (56 iterations) compared to deterministic (92 iterations) and stochastic (77 iterations) methods. The non-convex nature of the model necessitates careful selection of starting points to avoid local optimal solutions, which is addressed by transforming the primal problem into a linear program by fixing the integer variable. The LP problem is then efficiently solved using the Complex Linear Programming Expert (CPLEX) solver, enhanced by Monte Carlo simulations for 100 scenarios, achieving a 39.13% reduction in computational time. In addition to computational efficiency, this approach leads to operational cost savings of 25.02% by optimizing the selection of compressors (42.8571% decreased) and storage facilities. The model's practicality is validated through real-world simulations on the Belgian gas network, demonstrating its potential in solving large-scale hydrogen network transmission planning and optimization challenges.

1. Introduction

Hydrogen, increasingly recognized as an environmentally friendly fuel due to its potential to reduce CO_2 emissions [1], is gaining attention across multiple sectors including petroleum, chemical industries, fuel-cell vehicles, and energy production [2]. Traditional hydrogen production methods like fossil fuel-based reforming and coal gasification [3] are being complemented by innovative alternatives such as synthesis from organic waste and photoelectric water splitting [4–6], driven by a shift towards sustainable energy solutions. Currently, about 95 million tons of hydrogen are produced annually, mostly from natural gas [7,8], supporting sectors like refining and ammonia production. Hydrogen's role in the transportation and energy sectors is expanding [9], with technological advancements enhancing its production and applications [10–13]. Despite challenges, ongoing research into hydrogen's sustainable production and applications in areas like green hydrogen generation, refining, and steel production [9] offers promising prospects for reducing dependency on fossil fuels and minimizing environmental impacts [11,13].

In recent years, the concept of sustainable and fully integrated networks has gained significant interest from both policymakers and researchers [14]. This shift is driven by escalating costs, the need for sustainability, and advances in digital technology, prompting the evolution of isolated systems into cohesive, networked structures. These integrated systems deliver diverse services across various sectors, including transportation [15–17], electricity, water [18–20], and natural gas. Historically, these networks operated independently within their respective domains. Yet, they have grown increasingly interconnected due to shared goals of sustainability and cost-effectiveness. For instance, New England's electric power grid heavily depends on natural gas not only for electricity generation but also for heating residential buildings.

As a result, the complex and varied interdependencies among these network systems underscore the need for precise and sustainable network operations. Such operations would facilitate optimal management through a holistic approach, effectively balancing trade-offs [14,21].

* Corresponding author.
E-mail address: Muhammad.rasheed@uah.es (M.B. Rasheed).

https://doi.org/10.1016/j.est.2025.117840
Received 28 May 2024; Received in revised form 2 January 2025; Accepted 21 July 2025
Available online 7 August 2025

Nomenclature

Number Sets

$j \in \mathcal{J}$	index of junctions
$n \in \mathcal{N}$	index of compressor stations
$r \in \Re$	index of H_2 supply sources
$s \in \mathcal{S}$	index of H_2 storage units
$t \in \mathcal{T}$	index of time horizon

Other Symbols

δ'	variable discharge and suction pressure
$\acute{n}$	Hazen–Williams and Darcy-Weisbach component
α_n	loss at each node (n)
β_{cp}	compression loss at compressor (c)
δ	H_2 flow probability
ℓ	represents total no. of branches
η	variable operating cost factor
γ, k	are constants
$\mathbf{F}_{ab}$	total flow
$\mathbf{H}_{ab}$	nodal head of a pipe
$\mathbf{H}^p_{b,r}$	required pressure at the nodal head of a pipe
$\mathbf{H}^p_b$	pressure at nodal head of a pipe
$\mathbf{R}_{ab}$	resistance of a pipe
C_ℓ	pipeline capital cost
C_{cap}	capital cost
C_{op}	operating cost
$\mathcal{L}_m$	denotes length of a H_2 pipe in (km)
S_g	H_2 gas storage unit
$\mathfrak{d}$	denotes the internal diameter of a H_2 pipe in (mm)
$\overline{\gamma^t}$	storage level increasing over t
$\overline{v^t_g}$	max. the volume of a gas
$\overline{S_{g,v}}$	max. volume at storage unit
ψ_{S_n}	shutdown state of the compressor unit
σ_S	storage state at time t
$\underline{\gamma^t}$	storage level is decreasing over t
$\underline{\mathbf{H}^p_b}$	min. pressure at the nodal head of a pipe
$\underline{S_{g,v}}$	min. volume at storage unit
$\overline{\varphi_{S_n}}$	startup state of the compressor unit
ξ_{S_n}	on/off state of the compressor unit
a, b	nodes carrying non-zero flow
f	denotes the friction factor
$f_{a,b}$	H_2 flow from node a to b
fr_{ab}	friction of a pipe
$g_{d,t}$	H_2 demand over t
$H^t_{S_g}$	pressure head at the outlet of the storage unit
n_g	total no. of H_2 gas pipes
p	denotes gas pressure
p_a	denotes atmospheric pressure in psia
p_d	discharge pressure (psi)
p_s	suction pressure (psi)
PD	denotes pressure drop in the pipe
q_h	denotes volumetric flow rate in m^3/h
q_r	flow of H_2 gas supply sources
q_{in}	in-flow of a H_2 gas
q_{out}	out-flow of a H_2 gas
q_{st}	flow from storage facility
S_g	denotes relative density of gas
s_T	suction temperature
S_{ab}	cross-section area of a pipe
T	denotes temperature in °K
v^t_g	volume of a H_2 as in MMCFD
W	rate of work done
z	compressibility factor
$S_{g,v}$	volume at storage unit

Consequently, there is a pressing need for robust, dynamic, and autonomous modelling strategies. These strategies must accurately represent the diverse interdependencies of these systems while ensuring a flexible and scalable implementation across different application domains [22]. This research makes significant contributions to the field of hydrogen gas transmission network optimization by addressing the complexities of interdependencies, cost factors, and operational constraints.

This study extends traditional gas transmission models [23] to the hydrogen sector by developing a comprehensive and adaptive optimization framework that incorporates dynamic gas flow rates, pipeline design, storage capacities, and compressor costs. The primary contributions lie in employing a hybrid Mixed Integer Non-Linear Programming (MINLP) approach, integrating uncertainty through 100 scenarios in the Monte Carlo method, which dynamically adapts to fluctuating conditions. By transforming the non-convex optimization problem into a more tractable Linear Programming (LP) formulation via fixed integer variables, the model achieves a 39.13% reduction in computational time compared to conventional methods. Additionally, the novel algorithm yields a 25.02% reduction in operational costs through optimal compressor and storage selection. Rigorous real-world validation using Belgium's natural gas network highlights the model's practical applicability and robustness, marking a significant advancement in hydrogen network optimization by addressing both computational efficiency and cost minimization in dynamic and uncertain environments. The remaining paper is organized as follows.

Section 2 describes the related works. The system model and preliminaries are discussed in Section 3. The problem formulation is discussed in Section 4. Section 5 describes the solution methodology, algorithms, their implementation, and possible drawbacks. Simulation results are discussed in Section 6. Finally, the conclusion and future work are summarized in Section 7.

2. Related work

In the literature, optimization algorithms for hydrogen network operations often rely on formal graph-theoretic approaches and are tailored to specific applications. For example, a minimum-cost flow model was developed by Rabiee et al. [24] to optimize hydrogen transmission networks under uncertainty, using mixed-integer programming to minimize operational costs, but this approach does not fully account for network heterogeneity. The challenge arises because different types of system functions (such as pipeline capacities, gas flow variations, and storage requirements) introduce significant heterogeneity, which complicates optimization efforts. Traditional graph-based models, which consist of vertices (nodes) and edges (links), typically describe the topology of a network but fail to capture the dynamic processes or the varying nature of hydrogen flow under different scenarios.

Efforts to address these complexities have led to the development of multi-layer network frameworks. For instance, Liu et al. [25] proposed a tensor-based framework for modelling multi-layer energy systems,

including hydrogen networks, allowing for the integration of various network layers (such as pipelines, junctions, and storage facilities) to capture interdependencies and dynamic processes. However, while such models offer a more comprehensive understanding of complex systems, they often lack empirical validation in real-world scenarios, which limits their practical application. Other researchers, such as Hosseini et al. [26], have sought to expand upon traditional graph theory to better incorporate heterogeneity in energy networks, especially for hydrogen transportation systems. Their work provides a conceptual framework for modelling and analysing such systems, but it mainly focuses on theoretical formulations without substantial empirical data or simulations to validate the proposed models. Nevertheless, Kivelä et al. have outlined the modelling limitations that can be addressed with multilayer networks [27]. Consequently, solutions based on optimization algorithms may encounter these inherent limitations. Kivelä et al. have also introduced a convex energy-like function for modelling gas transmission systems involving pipelines and compressors [28], tackling some of these challenges.

It enables precise tracking of gas flow solutions through simple convex optimization. The approach also establishes a reliable gas flow model under uncertainties, validated through simulations for different gas transmission systems. However, this work has limited applicability to hydrogen network transmission planning, as it focuses on gas transmission systems. It also lacks a comprehensive exploration of uncertainties in the gas flow model and their impact on system feasibility. Additionally, the absence of real-world validation and case studies specific to hydrogen network transmission systems hinders its practicality. Qikun Chen et al. [29] proposed a work utilizing linepack as a gas storage buffer, these stations can operate compressors flexibly to minimize operational costs under varying electricity prices. The study demonstrates significant reductions in operational costs and emissions over 20% and 50%, respectively, and assesses the economic feasibility of investing in electric-driven compressors, sensitive to future carbon prices. However, the scope of this work is limited to Great Britain's gas network, which may raise questions about its generalizability to other networks. Furthermore, the focus on only the economic feasibility overlooks explicit consideration of environmental and safety aspects.

Moreover, the practical challenges and constraints related to real-world implementation in hydrogen gas transmission systems are not thoroughly addressed, necessitating further investigation for practical validation. Khalil et al. [30] present an optimization-based method for designing a hydrogen pipeline network, utilizing the existing natural gas network as a basis and allowing pipeline conversion. The approach achieves a 5.87% cost reduction compared to the initial solution and aligns with the potential hydrogen network, Wasserstoffnetz 2030, validating its effectiveness. However, the potential limitation of this work is that the optimization model might be limited by its reliance on certain assumptions and simplifications, which may not fully capture the complexity and variability of real-world scenarios. Further studies and considerations might be needed to address other factors, such as system reliability, and potential regulatory constraints, to ensure the feasibility and effectiveness of the hydrogen pipeline network design.

Sai Krishna et al. [31] present a nonlinear optimal control problem for intraday gas pipeline network operation, including storage reservoirs. It models gas flow dynamics in pipes, compressors, reservoirs, and wells using spatial discretization and coupled partial differential and nonlinear differential–algebraic equations. The objective is to maximize economic profit and network efficiency while respecting operating limitations. The proposed methodology is validated through computational experiments on pipeline test networks, demonstrating its effectiveness. However, the proposed work has limitations related to the representation of storage reservoir dynamics and the scalability of the solution method for larger networks. Adarsh et al. [32] used a multi-objective ant colony optimization strategy to minimize operating costs in a natural gas pipeline grid. It considers competing objectives of reducing fuel usage in compressors and increasing throughput at distribution centres. The methodology provides optimal solutions for each fuel consumption level on compressors and generates a Pareto front for gas distribution points, aiding pipeline managers in cost-effective operation. However, this work focuses solely on optimizing the operating costs of the natural gas pipeline grid using the ant colony optimization strategy. Further research would be needed to explore the broader implications and potential trade-offs involved in optimizing natural gas pipeline grids. Chongyuan Shui et al. [33] present a work that applies optimal transport theory to optimize natural gas pipeline operations, considering line-pack effects. The problem is divided into two stages for solvability with existing methods. The proposed model demonstrates effectiveness, achieving a 14.5% energy saving in the studied pipeline segment. However, the main limitation of this work is its focus on optimizing the network while overlooking certain complexities and comprehensive modelling features. Additionally, its applicability to large-scale networks and integration with other energy systems may need further investigation.

Farid [34] identified that a graph theory-based modelling approach has also been used in a generalized multi-commodity network flow optimization. Although this approach has implemented a notion of function heterogeneity, however, it does not integrate a specific state and description of the operands and storage units. Finally, the developed strategies used to optimize the discipline and application-specific integrated solutions lack general ability. Furthermore, this work lacks empirical validation or practical case studies to demonstrate the effectiveness and applicability of the proposed composite reconfigurability measures in real-world manufacturing systems. To further overcome these limitations, a hetero-functional graph theory (HFGT) was introduced to study the reconfigurability of network systems [17,35,36] and has already been applied to solve several sizeable, flexible engineering systems. These include; electric power grids, water distribution systems, transportation networks, healthcare management systems, and other interdependent infrastructures. Schoonenberg and Fard [22] have further developed an HFGT to include a tensor-based formulation to introduce system flexibility. Generally, an HFGT has introduced many modelling constructs not found in the traditional graph theory approach [37].

The limitations in existing optimization strategies for hydrogen flow networks stem from their focus on gas networks, which lack applicability to hydrogen systems due to differences in storage and flow dynamics [27]. Many models, such as those by Khalil et al. [30] and Qikun Chen et al. [29], rely on simplifications like using natural gas infrastructure, limiting their generalizability and robustness in real-world scenarios. Additionally, these studies inadequately address uncertainty in flow dynamics, environmental impacts, and safety concerns [27,29], which are critical for hydrogen networks. Most approaches also lack real-world validation, particularly in large-scale networks [31,32], and face challenges with scalability [33], highlighting the need for more flexible and validated models that can handle the unique complexities of hydrogen transmission.

3. System model

This section explains the preliminaries of the study, the system model and its layout, the mathematical models of H_2 gas flow rate, the storage model, the objective function, and the constraints [23,30,33,38].

3.1. Test case selection

For implementation, Belgium's gas network (Fig. 1) is selected for this study due to its strategic importance, publicly available dataset and comprehensive infrastructure, which provides a well-balanced test case for hydrogen transmission optimization. Because, Belgium's gas network is characterized by a combination of high-and-low-gas pipelines, compressor stations and their locations, and storage units, making it

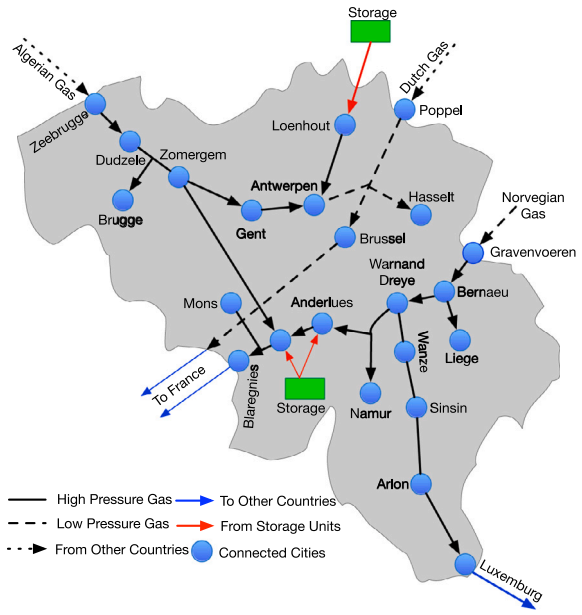

Fig. 1. Schematic diagram of the low and high-pressure Belgium Gas Network, highlighting the 13 nodes (Table 2) and the corresponding flow directions.

an ideal representation of regional & transnational gas flows. This network also serves as a transit hub for natural gas between multiple European countries, such as France, Netherlands, Norway, Luxembourg and Germany. Eventually, this makes the Belgian network a complex yet practical case for hydrogen conversion, ensuring that the results can be generalized and adapted to other networks within Europe. Additionally, the geographic location of Belgium has established connections to other gas sources such as Dutch, Algerian, and Norwegian gas, which make it particularly suitable for investigating the dynamic interplay of hydrogen transmission, storage, and distribution in a real-world, heterogeneous network setting.

3.2. Preliminaries

This work focuses on the Belgium gas distribution network depicted in Fig. 1, highlighting key design and operating factors such as the total number of nodes, storage unit supply locations, and destination nodes. The network is engineered to transport a predetermined quantity of H_2 gas from single or multiple points to others, with well-defined initial and final states (i.e., supply pressure, composition, temperature). It consists of several key nodes categorized by their roles. The high gas nodes include Gravenvoeren, Liege, Namur, Sinsin, Arlon, Mons, Blarengies, and Anderlues. The low gas nodes are Zeebrugge, Poppel, Hasselt, and Brugge. Additionally, there are gas storage units near Antwerp and Blarengies. The network also features connected cities such as Antwerp and Luxembourg, with flow directions indicated for exports to France and other countries.

We have considered this Belgium gas network as a model for our hydrogen gas network (Fig. 1) that consists of supply sources ($r \in \Re$), set of compressor units ($n \in \mathcal{N}$), storage units ($s \in S$), junctions ($j \in \mathcal{J}$) and flow networks. These networks are composed of a storage facility, arcs & nodes (a, b) of pipeline network, compressor units, and distribution sites. The optimal design of a transmission and distribution network involves capital expenditures, operational & maintenance costs, depreciation costs, and return on investment (ROI), respectively. Before designing these networks, various parameters must be considered to ensure optimal operation:

- *Required pressure*: to ensure the required gas pressure at distribution locations, determining the optimal number and location of compressor units becomes crucial within a given time horizon.
- *Network design*: when the initial network design allows for potential expansion based on future requirements, obtaining the optimal solution for the extended design is essential to achieve cost-effective expansion and operation.
- *Network parameters*: the design of single or interconnected networks should include optimal parameters such as diameter, length, number of nodes, and arcs to manage gas pressure at the supply side effectively.
- *Initial conditions*: during implementation, certain parameters are fixed, such as the initial discharge pressure and flow rate at the Gravenvoeren node (Fig. 1) is fixed at 500 psi and 600 MMCFD, which vary over time with changes in demand. Similarly, pipeline length and diameter in all branches are fixed (Table 3), while the flow across nodes is adjusted to meet the demand.
- *Flow condition*: The steady-state equations presented in Section 3.3 are designed to model gas flow while focusing on optimizing the gas network's cost parameters, including capital cost, operating cost, pipe capital cost, compressor annual cost, and the selection of optimal compressors, length & diameter of pipe to meet demand requirements (see Table 1). This model also integrates fixed storage (10% of total demand) considerations within the operating time interval (unit time), which allows for a simplified representation of storage behaviour in steady-state conditions.
- *Boundary conditions*: the optimization program incorporates these conditions and a set of constraints as detailed in (Sections 3.3, 3.4, 3.7 and 3.8) to obtain globally optimal results, achieving minimal cost and computational complexity.

Based on these parameters, a cost minimization objective function is formulated to determine (i) the total number of compressor units, (ii) the length of supply and distribution pipeline segments, (iii) the diameter and length of pipelines, and (iv) the supply and discharge pressure at each compressor unit.

The primary objective of this study is to minimize costs over one year, accounting for maintenance, capital, and operational costs. The design challenge does not constrain the number of compressor units or locations, lengths of pipeline segments, diameters of pipes connecting different branches, or locations of branching points. Thus, the objective function is modelled as a mixed integer nonlinear programming (MINLP) problem. Before detailing the proposed network layout, it is crucial to distinguish between two optimization problem types. First, if the total cost of the H_2 gas compressors is a linear function of horsepower, the problem can be addressed using nonlinear programming (NLP). Alternatively, suppose the total cost includes a fixed capital component for zero horsepower. In that case, the problem becomes more complex and is better handled using branch-and-cut or branch-and-bound algorithms. While these approaches can provide optimal results, they might also increase the system's complexity if the objective function and constraints are not precisely defined. The problem formulation encompasses several aspects: (i) the H_2 gas flow rate, (ii) the pipeline configuration design, (iii) the control and design variables, (iv) the cost minimization objective function, and (v) the equality, inequality, and binary constraints.

3.3. Gas flow rate

Generally, the common way to express a gas flow rate (q_g) using the Weymouth Equation in terms of cubic meter per hour (m^3/h) at standard conditions for isothermal flow is written as [39,40] in Eq. (1):

$$q_g = 1.361 \times 10^{-7} \sqrt{\frac{p_d^2 - p_s^2}{f.\mathcal{L}_m.T.S_g}\mathfrak{d}^5} \tag{1}$$

where p denotes gas pressure (psi), T denotes the temperature in (°K), S_g denotes the relative density of the gas in (0.005229 lb/ft3), [28], $\mathcal{L}_m$ is the length of a pipe in (km), $\mathfrak{d}$ denotes the internal diameter

of a pipe in (mm), and f is the friction factor which depends on the material. However, other equations like Weymouth and Panhandle can also be used to express the gas flow in long pipelines. It is also assumed that the hydrogen flow rate is unidirectional in each pipe as denoted by Eq. (2):

$$q_h^t \geq 0;\ \forall n_g, t \in \mathcal{T}, \tag{2}$$

For high-pressure and long pipes, the Weymouth equation is most widely used due to efficiency and is written as follows in Eq. (3):

$$q_h^t = (2.61 \times 10^{-8}) \times d^{2.667} \sqrt{\left[\frac{p_d^2 - p_s^2}{f.\mathcal{L}_m.S_g}\right] \frac{288}{T}}, \forall t \in \mathcal{T} \tag{3}$$

where p_d&p_s denote discharge and suction pressure, while friction factor in Eq. (3) is $f = \frac{0.094}{d^{1/3}}$. Furthermore, this friction factor is the same as obtained from the Moody diagram [41] for the 20-inch pipeline. However, the friction factor is larger for smaller than 20-inch diameter pipe and vice versa. To calculate the pressure drop (ζ in %) over t in pipe n_g, the following expression can be used that is presented in Eq. (4),[23]:

$$\zeta_{ng}^t = \left(\frac{p_d^t - p_s^t}{p_d^t - p_a^t} \times 100\right), \forall t \in \mathcal{T} \tag{4}$$

where $p_a = 14.73$ psia denotes the atmospheric pressure.

3.4. Pipeline design

Fig. 1 shows the considered network layout & configuration and notations employed for the compressors in terms of nodes, and the H_2 gas pipeline segments. An interconnected node can either represent each compressor unit and an arc represents each pipeline. Let $n \in \mathcal{N}$ represent the total number of possible compressor stations in each branch $\ell = 3$. Let the set of possible junctions denoted by $|j| = \mathcal{J}$, while the fixed or dynamic gas demand $g_{d,t}$ over time interval t is applied over the junction(s) ($j \in \mathcal{J}$). It is also assumed that the value of the gas demand $g_{d,t}$ is known in advance for the junctions $j \in \mathcal{J}$ and $t \in \mathcal{T}$. Let a, b denote the gas pipes/nodes that carry the non-negative flow $q_{a,b}$ from node a to node b. When the gas distribution network is designed, it is equally important to ensure gas flow continuity (i.e., gas supply - gas demand = 0); since the pressure increases at the compressor unit and decreases along the junctions. Therefore, the consideration of the gas pressure drop/loss factor must also be ensured across all the junctions in the network. In addition, the H_2 transmission and distribution network is assumed to be horizontal. For each pipeline configuration, every node and arc is labelled, separately. For example, total number of compressors $n = \sum_{t=1}^{\mathcal{T}} \mathcal{N}^t$, the initial suction pressure $p_{s,n}$ at $t-1$, the discharge pressure $p_{d,n}$, and the length of the pipeline segment $\mathcal{L}$ and respective diameter $\mathfrak{d}(n+1)$. The gas demand flow balance at junction $j \in \mathcal{J}$ is represented by the Eq. (5), while the inflow and outflow must always be equal to meet the demand capacity over the given time.

$$g_d^t = \sum_{t=1}^{\mathcal{T}} \sum_{a \in q_{in}(b)} q_{ab}^t + \sum_{c \in q_{out}(b)} q_{bc}^t,\ \forall t \in \mathcal{T}, \tag{5}$$

where, $a \in q_{in}(b)$&$c \in q_{out}(b)$ denote the nodes supplying and carrying gas flow from junction b (i.e., $a \rightarrow b$ and $b \rightarrow c$). The steady-state gas flow equation over time ($t \in \mathcal{T}$) can be written as Eq. (6):

$$\sum_{t=1}^{\mathcal{T}} \left\{ \left(\delta q_{ab}^t + \sum_{n=1}^{\mathcal{N}} \alpha_n^t \right) - \left(\sum_{r=1}^{\Re} q_r^t + \sum_{s=1}^{S} q_{st}^t + \sum_{n=1}^{\mathcal{N}} \beta_{cp}^t \right) \right\} = 0, \forall t \in \mathcal{T}, \tag{6}$$

where δ denotes the probability to analyse uncertainty in the networks optimization problem, α_n^t denotes loss due to internal friction, β_{cp}^t represents the compression loss over time t which is due to the working of a compressor, and q_r^t denotes the flow over t at supply resources, q_{st}^t denotes the flow at storage sources over t, respectively.

$$(\xi_n^{t-1} + \varphi_n^t - \psi_n^t) - \xi_n^t = 0, \forall n, t, \tag{7}$$

Eq. (7) denotes the switching states of the hydrogen compressor unit.

$$\mathbf{F}_{ab} = \sum_{t=1}^{\mathcal{T}} \sum_{\forall n_g} \left\{ q_{ab}^t + g_d^t \right\},\ \forall\ t \in \mathcal{T}, n_g, \tag{8}$$

Eq. (8) shows the gas flow balance ($\mathbf{F}_{ab}$), n_g denotes the number of pipes, q_{ab} denotes the gas flow from node a to b and g_d^t denotes the H_2 demand over a given time interval. $\mathbf{H}_a$ and $\Re_{ab}$ denote the nodal head and the coefficient of resistance in Eq. (9), while the $\tilde{f}$ defines the exponent of the flow. The H_2 gas flow balance is denoted by Eq. (9), [42–47].

$$\mathbf{H}_a - \mathbf{H}_b = \Re_{ab} q_a |q_b|^{\acute{n}-1}, \tag{9}$$

Eq. (9) denotes the pressure head loss across all pipelines. It is further assumed the system operator has control over the minimum pressure $\underline{\mathbf{H}_b^t}$ to fulfil the flow demand at all junctions j. Let $\mathbf{H}_b^t$ denote the current pressure head to satisfy the required head level $\underline{\mathbf{H}_b^t}$ at time t (Eq. (10)).

$$\mathbf{H}_b^t \geq \underline{\mathbf{H}_b^t}, \tag{10}$$

where the gas flow among all the nodes is denoted by Eq. (11).

$$q_{ab} = \frac{\mathbf{H}_a - \mathbf{H}_b}{\Re_{ab}^{0.54} |\mathbf{H}_a - \mathbf{H}_b|^{0.46}}. \tag{11}$$

$$\mathbf{H}_{j,t} \geq \underline{\mathbf{H}_j},\ \forall\ j \in \mathcal{J}, n_g, \&\ t \in \mathcal{T} \tag{12}$$

Eq. (12) denotes the minimum allowable flow over t must satisfy the pressure head $\mathbf{H}_j$. It is defined as $\underline{\mathbf{H}} = \{\mathbf{H}_j | j| \in \mathcal{J}\}$ and $\mathbf{G} = \{G_{d,t} | j| \in \mathcal{T}, t \in \mathcal{T}\}$. Here, the optimal selection of pressure head loss depends on the optimal selection of ń in Eq. (9). The Hazen–Williams and Darcy-Weisbach with ń = 1.852 and ń = 1.852 relationships are being widely adopted for pressure head calculation [46,47]. Both the Hazen–Williams and Darcy-Weisbach relationships can be alternatively used to calculate pressure head loss. However, the former involves less complex calculations as compared to the latter one. Similarly, the head loss ℓ_{ab}^t of pipes (ab) carrying non-zero flow at time instant t can be computed using Darcy Weisbach Eq. (13):

$$\ell_{ab}^t = \mathbf{F}_{ab} \times (q_{ab}^t)^2, \forall t \in \mathcal{T} \tag{13}$$

where, $\mathbf{F}_{ab}$ is a constant having non-negative value which is equal to $\frac{q_{ab}\ell_{ab}}{2d_{ab}S_{ab}^2 g} \geq 0$. Where l_{ab}&d_{ab} denote the length and diameter of the pipe (in meter), g is the acceleration of gravity (in m/s^2), and S_{ab} represents the cross-section area of the pipes. At each time $t \in \mathcal{T}$, pressure head H must satisfy the constraint of Eq. (14):

$$0 \leq \underline{\mathbf{H}_j} \leq \overline{\mathbf{H}_j} \tag{14}$$

where, $\underline{\mathbf{H}_j}$ and $\overline{\mathbf{H}_j}$ denote the minimum and maximum head at j over time interval t. Thus for each junction J, the values of H can be defined as; $\underline{\mathbf{H}} = H_j | j \in \mathcal{J}|$.

Furthermore, the H_2 supply tanks and/or reservoirs can be modelled by considering the volume of gas at a certain time. Let the volume H_2 in the supply tanks be denoted by v_g^t. Then the supply balance constraint at time t is written as Eq. (15):

$$v_g^t = v_g^{t-1} + q_{ab}^t \tag{15}$$

$$0 \leq v_g^t \leq \overline{v_g^t} \tag{16}$$

Eq. (16) establishes the lower limits on the volume of H_2, and the variable $\overline{v_g^t}$ represents the maximum allowable volume of H_2 at time t. Algorithm 1 explicitly details the gas flow management process, dynamically adjusting the flow based on real-time demand (p_d^t). This

algorithm provides a responsive mechanism to balance hydrogen production and storage with consumer and industrial needs, thereby optimizing operational efficiency and reliability. Integrating these elements within our model highlights the interdependencies between supply limits and demand fulfilment, underscoring the complexity of efficiently managing hydrogen distribution networks.

Algorithm 1: Hydrogen Flow Procedure based on Demand Capacity.

Input: t, n, g_d^t
Output: $\mathbf{F}_{ab}$
if $g_d^t \le q_{ab}^t + S_{g,v}^t$ **then**
  $q_{ab}^t = q_{ab}^t - S_{g,v}^t$ & $S_{g,v}^t$ *has* $\overline{\gamma^t}$ state **else if** $g_d^t > q_{ab}^t$ **then**
    $q_{ab}^t = q_{ab}^t + S_{g,v}^t$ & $S_{g,v}^t$ *has* $\underline{\gamma^t}$ state
    else if $q_{bc}^t \le S_{g,v}^t$ **then**
      $q_{ab}^t = q_S^t$
    end
  end
end

3.5. Pump model

Hydrogen pumps consume energy to elevate the nonzero ($\underline{\mathbf{H}_j} - \underline{\mathbf{H}_i} \ge 0$) head along the pipes n_g over time t, given by Eq. (17),

$$\underline{\mathbf{H}_j} - \underline{\mathbf{H}_i} \le A_{i,j}(q_{i,j}^t)^2 + B_{ij}(q_{i,j}^t) + C_{ij}^t \tag{17}$$

where, $A_{i,j}$, B_{ij} and C_{ij} are positive constants of a quadratic cost function that supply electric power to the pumps on each pipe over time t.

3.6. Pressure valves

The hydraulic head pressure is changed due to minimum pressure requirements $\mathbf{H}_r^t$ along pipes (n_g) over given time t as given below:

$$\mathbf{H}_j - \mathbf{H}_i = \mathbf{H}_{b,r}^{p,t}, \forall t \in \mathcal{T} \tag{18}$$

3.7. Storage model

In this paper, each storage unit is modelled as a node integrated across the network. Let S_g represent the H_2 storage facility and $S_{g,v}^t$ indicate the volume of H_2 in each facility at time t. The H_2 balance constraint at each storage facility for any time t is expressed by Eq. (19), which ensures that the difference between the inflow $a \in f_{in}(b)$ and outflow $c \in f_{out}(b)$ at node "b" remains constant over the specified time interval.

$$S_{g,v}^t = S_{g,v}^{t-1} + \left(\sum_{a \in f_{in}(b)} \mathbf{F}_{ab}^t - \sum_{c \in f_{out}(b)} \mathbf{F}_{b,c}^t \right), \forall t \in \mathcal{T} \tag{19}$$

$$\underline{S_{g,v}^t} \le S^t{}_{g,v} \le \overline{S_{g,v}^t} \tag{20}$$

Where, the variable $S_{g,v}^{t-1}$ denotes the volume of H_2 in $t-1$ time slot. The upper $\overline{S_{g,v}^t}$ and lower $\underline{S_{g,v}^t}$ limits on the H_2 storage facility are denoted by Eq. (20). Consequently, Eq. (21) denotes the state equation of the storage unit.

$$S_0^t = \sigma_S, \forall S, t = 0, \tag{21}$$

For the pressure head at the outlet of the water storage facility, $H_{S_g}^t$ is modelled over time t based on water demand or flow capacity. Changes in the head at the storage valve relative to the gas volume are described by Eq. (22)

$$H_{S_g}^t - H_{S_g}^{t-1} = \left(\sum_{a \in f_{in}(b)} \mathbf{F}_{ab}^t - \sum_{c \in f_{out}(b)} \mathbf{F}_{b,c}^t \right), \forall t \in \mathcal{T} \tag{22}$$

3.8. Control variables

The pipeline segments shown in Fig. 1 have a different set of variables: (i) the volumetric H_2 gas flow rate ($Q_{a,b}$), (ii) the H_2 discharge pressure (psi) of the nth compressor ($p_{d,n}$), (iii) the suction pressure (psi) of nth compressor ($p_{s,n}$), (iv) the diameter ($\mathfrak{d}$) and length ($\mathcal{L}$) of the transmission network. Since, the mass flow rate is considered dynamic, which changes with the demand requirement. Therefore, the associated variables need to be evaluated for each segment over the given time t.

4. Problem formulation

This work aims to calculate the total cost, including both the operating and maintenance expenses of installed compressors and the capital cost (C_{cap}) of pipelines and compressors. Notably, each compressor is assumed to be adiabatic, with an inlet temperature that equals the ambient temperature. For analysis purposes, a lengthy segment of the Belgium gas network, starting at the Norwegian supply unit in Gravenvoeren (node 1, Fig. 1), is considered to maintain the ambient temperature before reaching the next nodes. Although the actual C_{cap} of each pipeline segment primarily depends on the diameter ($\mathfrak{d}$) and length ($\mathcal{L}$), this study simplifies the calculation by assuming a uniform cost of 870/inch/mile/year. Typically, the rate of work (W) performed by a single compressor is defined as shown in Eq. (23):

$$W_n = \gamma \times \tilde{q}_{a,b} \left(\frac{k}{k-1} \right) \times s_T \left[\left(\frac{p_{d,n}}{p_{s,n}} \right)^{z(k-1)/k} - 1 \right] \tag{23}$$

where γ is a constant valued at 0.08531, $\tilde{q}_{a,b}$ represents the non-negative dynamic gas flow rate under standard temperature conditions, $k = C_p/C_v$ for gas at suction condition is 1.41, z denotes the compressibility factor at suction conditions ranging from 1.0 to 1.05, and s_T refers to the suction temperature, set at 520 °K.

Yearly operating and maintenance costs for the compressors are generally linked to their capacity and are estimated to range from (8–14$/horsepower/year + 10,000$), covering installation, foundation, and other related expenses. Each compressor operates under specific equality and inequality constraints to ensure that the discharge pressure remains adequate relative to the suction pressure. Nonetheless, factors such as friction, leakage, and temperature variations often lead to pressure losses, making it challenging to maintain a consistent balance between discharge and suction pressures.

4.1. Pressure & compression constraint

This study imposed a constraint Eq. (24) so that a discharge pressure is always greater than or equal to the suction pressure [23].

$$0 \le p_{s,n}^t \le p_{d,n}^t, \forall n \in \mathcal{N}, t \in \mathcal{T} \tag{24}$$

$$0 \le \frac{p_{d,n}^t}{p_{s,n}^t} \le \overline{\left(\frac{p_{d,n}^t}{p_{s,n}^t}\right)}, \forall n \in \mathcal{N}, t \in \mathcal{T} \tag{25}$$

Eq. (25) denotes the compression ratio $\frac{p_{d,n}^t}{p_{s,n}^t}$ must be within maximum limit $\overline{\left(\frac{p_{d,n}^t}{p_{s,n}^t}\right)}$ for safe operation.

4.2. Constraint on limits

$$\underline{(1-\delta')p_{d,n}^t} \le p_{d,n}^t \le \overline{p_{d,n}^t} \tag{26}$$

$$\underline{(1-\delta')p_{s,n}^t} \le p_{s,n}^t \le \overline{p_{s,n}^t} \tag{27}$$

$$\underline{\mathcal{L}_n} \le \mathcal{L}_n \le \overline{\mathcal{L}_n} \tag{28}$$

$$\underline{\mathfrak{d}_n} \le \mathfrak{d}_n \le \overline{\mathfrak{d}_n} \tag{29}$$

Eqs. (26)–(29) set the lower and upper limits on demand, supply, length, and diameter variables. The variable δ represents the uncertainty in supply and discharge pressures. For implementation purposes, the length of the transmission network is held constant. Consequently, an equality constraint is applied to the transmission network, which consists of three branches (ℓ, Fig. 1), as follows:

$$\ell_n = \sum_{j=1}^{\mathcal{J}} \ell_j, \tag{30}$$

The total cost is now represented by Eq. (31):

$$\begin{aligned} C_t = & \sum_{t=1}^{\mathcal{T}} \sum_{n=1}^{\mathcal{N}} W_n^t + (\eta \times C_{op}^t) + C_{cap}^t + \sum_{t=1}^{\mathcal{T}} \sum_{j=1}^{\mathcal{J}} C_\ell^t \times \mathcal{L}_j^t \times \mathfrak{d}_j^t \\ & + \sum_{t=1}^{\mathcal{T}} \sum_{s=1}^{\mathcal{S}} S_{g,v}^t + (\overline{\gamma^t} + \underline{\gamma^t}) \end{aligned} \tag{31}$$

The cost reduction objective function (z) over a given time t for (j) and (s) is denoted by Eq. (32):

$$minz = \sum_{t=1}^{\mathcal{T}} C_t \tag{32}$$

subject to: Eqs. (5), (6), (9) to (16), (19), (20), (22) and (24) to (30) where C_{op}(\$/hp-year), C_{cap}(\$/hp-year), and C_ℓ(\$/in-mile-year) represent the yearly operating, capital, and pipeline costs, respectively. $\mathcal{L}_j$(mile) and $\mathfrak{d}_j$(in) specify the length and diameter of the pipeline segment, respectively. The variable η in C_{op} indicates that operating costs can vary based on other cost factors.

4.3. Uncertainties in Monte Carlo

The Monte Carlo method is implemented to incorporate and analyse the uncertainties in input data in $(p_d, p_s, \mathcal{L}, \overline{\mathfrak{d}}, ratio(\frac{p_{d,n}^t}{p_{s,n}^t}), q)$. The variation in parameters is captured by generating multiple scenarios. These parameters are varied within predefined bounds (±10% under normal distributions across 100 iterative scenarios.) The results from each scenario were then evaluated to analyse the overall system performance under uncertainty. The probabilistic outputs helped us estimate optimal solutions while accounting for variations in key parameters, thus adding robustness to the decision-making process regarding pipeline infrastructure and compressor selection.

5. Solution approach and methodology

The proposed system model consists of 13 nodes and a variable number of compressors (n), dynamically selected by the control algorithm during operation time (t) based on demand, supply pressure, and storage volume considerations. In the model shown in Fig. 1, the objective function can be solved using NLP algorithms when considering the capital cost in Eq. (31). In that case, solving the objective function requires branch-and-cut or branch-and-bound methods to handle the nonlinear control variables (Eqs. (13), (15), (23)). The branch-and-bound approach effectively reduces complexity by eliminating unnecessary solution sets. In this method, a tree structure is formed based on the network's nodes and branches, where each node represents an optimization problem (Eq. (31)) with or without integer variables. Node 1 in the proposed model represents the primal optimization problem, including the capital cost. The solution obtained at node 1 is a lower bound for the subsequent optimization problems involving the cost function. If the solution at node 1 is infeasible, the process is restarted. However, the solution is considered valid if feasible, even considering the initial capital cost at zero horsepower.

The proposed model is evaluated using different algorithms, including deterministic, stochastic, and dynamic approaches, to enhance the solution's effectiveness in analysing convergence and optimality. These methodologies were selected to highlight the efficiency of our dynamic optimization approach. We benchmarked it against deterministic and stochastic methods, both of which are standard in network optimization but have limitations in handling uncertainties and computational costs. Our method, incorporating Monte Carlo scenario analysis, outperformed these approaches, reducing computational time by 39.13% and operational costs by 25.02%. In the deterministic approach, the initial pressure at supply points (Eqs. (24)–(27)), flow, and cost are kept fixed during implementation. The problem is transformed into a LP formulation by fixing the integer variable, yielding an integer optimal solution. The initial solution (Mixed-Integer Programming - MIP) is achieved in 92 iterations, and the second solution (LP) is obtained in 77 iterations. During implementation, the operating cost of compressors (Eq. (31)) is observed as dynamic due to the behaviours of decision variables. For simulation purposes, a gas storage unit is integrated at node 9, adding complexity to finding an exact optimal solution. To address this challenge, we utilize a "discrete constraint optimization" strategy with a dynamic search method. The objective function is solved in 64 iterations to obtain an integer optimal solution, followed by fixing integer variables for solving second-stage LP problems as in the deterministic approach. The first-stage MIP is solved in 70 iterations, and the reduced LP problem is solved in 56 iterations. The overall objective function (Eq. (31)) is optimized using the CONOPT solver in 59 iterations. Finally, we implement a dynamic search algorithm to solve the network optimization problem considering dynamic flow, storage integration (Eqs. (19), (20) and (22)), and dynamic operating cost. The MIP and LP solutions are obtained in 66 and 65 iterations, respectively, both proven to be optimal. Notably, the NLP with discrete optimization strategy and CPLEX solver achieves faster convergence compared to the deterministic and stochastic strategies.

The optimization problem at node 2 is also nonlinear, with multiple compressors considered based on branch length. The decision tree in a network graph descends in each iteration, constraining the solutions until the global solution is obtained. The lower and upper bounds for each compressor in each respective pipeline remain constant. It is worth noting that the solution obtained at node n in a decision tree could be feasible but not necessarily optimal. Therefore, we may call it a viable or general solution. To ensure optimality, the implementation continues until the entire network is configured with reduced cost.

Finally, in the context of gas network optimization using graph theory modelling, a combination of these approaches might be most effective. A dynamic approach captures time-dependent aspects, a stochastic approach handles uncertainty in demand and supply, and a deterministic approach finds precise solutions for certain fixed conditions. The specific trade-offs between accuracy, computational complexity, and ability to handle uncertainty will guide the choice of the most suitable approach or combination of approaches. It is essential to consider the problem's characteristics and optimization objectives before deciding on the methodology.

Throughout the paper, all variables are defined with their values. The following assumptions are made in this work:

- *Demand Capacity*: the value of the gas demand (g_d^t) is known in advance for the set of junctions ($j \in \mathcal{J}$) over a given time $\mathcal{T}$.
- *Flow Rate*: nodes "a" and "b" denote the nodes that carry the non-negative flow ($q_{a,b}$) of gas from node "a" to node "b".
- *Supply-Demand Ratio*: the gas distribution network is designed with an initial assumption that gas supply and demand are zero during the operation time. This is ensured through the optimal solution.
- *Network Layout*: the gas transmission and distribution network is assumed to be horizontal.
- *Network Length*: the initial length of the distribution network is fixed, however, the optimization algorithms optimize the length and diameter to minimize the overall cost as detailed in Table 3.

5.1. Major challenges and simplifications of the model

This section describes the major challenges and their simplifications in solving the gas network optimization problem. These can be enumerated as follows:

- *Pressure and Flow Characteristics*: hydrogen gas exhibits varying pressure and flow characteristics over time, especially when demand is dynamic. Thus, the network must be designed to meet demand requirements without losing pressure. We address this by considering dynamic gas flow rates (Eqs. (1), (3) to (6) and (8)). The demand capacity varies over time, and pressure drop (Eqs. (4), (27) and (28)) is implemented as a constraint to maintain the supply–demand ratio (Eqs. (25) and (27)) during the implementation process. Additionally, pipeline design ensures the nodal head pressure is maintained (Eq. (9)–Eq. (16)) over time.
- *Demand Management*: storage units allow for decoupling production and consumption rates. Excess capacity can be stored for later use during low-demand or high-production periods, ensuring a stable and reliable supply. Coordinating production and storage is critical to avoid wastage and inefficiencies. Matching supply and demand with storage capacity is complex, especially with intermittent renewable energy sources. This problem is modelled in Section 3.7 and considered a constraint in solving the objective function (Eq. (24)).
- *System Modelling Complexity*: integrating storage into the multi-objective optimization model may increase the system modelling complexity. Handling multiple parameters, constraints, and objectives related to storage can be challenging for the optimization algorithm. Therefore, the mathematical models are designed to ensure a globally optimal solution without violating any constraints.
- *Feasibility & Practicality of Proposed System*: it is also equally important to ensure the feasibility of using existing natural gas pipelines to transport pure hydrogen. Recent studies and reports, including those by the European Hydrogen Backbone Initiative (EBH) [48] and Gas for Climate (2020) [49], confirm the practicality of repurposing natural gas infrastructure for hydrogen transmission. It is generally feasible to use existing pipelines with minimal modifications for low-pressure hydrogen networks. However, high-pressure networks may require adaptations such as material upgrades and compression technology enhancements due to hydrogen's smaller molecule size and potential for embrittlement in steel pipelines [50]. For example, the UK's HyNet Northwest project has demonstrated the successful retrofitting of natural gas pipelines for hydrogen transport under real-world conditions [51,52]. Furthermore, the EHB study provides a roadmap for transitioning existing gas networks to accommodate hydrogen by 2040, validating the practicality of such approaches across multiple European countries, including Belgium EHB.

6. Results and discussion

In the proposed system model (refer to Section 3), we apply our approach to the Belgium gas network (Fig. 1), a network comprising 13 nodes, including a single supply point and a storage unit. This particular network was selected for its variability in gas demand across different nodes (such as Luxemburg, Blaregnies, and Liege), which effectively represents realistic usage patterns. Additionally, the variation in demand ratios over a specified period, t, is involved in demonstrating the model's convergence rate. Table 1 provides the variables and their values used in this implementation, while Table 2 lists the nodes alongside their corresponding city names.

The flowchart in Fig. 2 provides a detailed step-by-step process for optimizing the hydrogen network transmission. The process begins with setting the number of iterations, which defines the total computational runs for optimization. Next, the initialization of variables, such as flow rates, demand profiles, and key parameters for pipelines, compressors, and storage, is performed. After this, the objective function, constraints, and limits are established to minimize both computational and operational costs. The solver selection follows, where the GAMS system, using the CONOPT solver, is employed due to its effectiveness in handling large-scale, non-linear optimization problems common in gas network planning. Once the problem is solved, the solution is checked for optimality. If the solution is not optimal, the model loops back, adjusting variables as necessary. If an optimal solution is found, the model proceeds to Monte Carlo simulation with uniform distribution for scenario analysis, which tests the robustness of the solution under uncertain conditions (e.g., fluctuations in demand or supply). If the solution still proves to be optimal after scenario analysis, the results are saved. Otherwise, adjustments are made, and the problem is resolved. The loop continues until the total iterations are exhausted or the stopping criteria (such as convergence or stability of the solution) are met. The iterative and scenario-based process ensures that the final solution is both computationally efficient and operationally feasible, which is critical for the real-world application of transforming Belgium's natural gas network into a hydrogen network.

Based on the system model shown in Fig. 1, the solution results of the designed problem are illustrated in Figs. 3 to 7. In Fig. 3, the discharge pressure across the various nodes in the network is compared for three different approaches: deterministic, stochastic, and dynamic. The results show that the proposed dynamic approach exhibits superior performance in terms of discharge pressure optimization. The key advantage of the dynamic approach lies in its ability to respond to

Table 1
Simulation variables.

Variable	Meaning	Value
k	suction condition	1.41
z	compressibility factor	1.00
s_T	suction temperature	60 °C
η	compressor cost	70 ($/hp/year)
C_l	pipe capital cost	870 ($/inch/mile)
C_{op}	operating cost	8 ($/hp)
p_s	suction pressure	198.4 (psi)
$\overline{p_s}$	max. suction pressure	1000 (psi)
$\underline{p_s}$	min. suction pressure	200 (psi)
$\overline{p_d}$	max. discharge pressure	1000 (psi)
$\underline{p_d}$	min. discharge pressure	200 (psi)
$\overline{q}$	max. discharge pressure	600 (psi)
$\underline{q}$	min. discharge pressure	200 (psi)
$\overline{\mathfrak{d}}$	max. diameter of pipe (initial)	36 (inch)
$\underline{\mathfrak{d}}$	min. diameter of pipe (initial)	3 (inch)

Table 2
Nodes and corresponding cities in the Belgium gas network.

Node	City
1	Gravenvoeren
2	Bernaeu
3	Liege
4	Warnand Dreye
5	Wanze
6	Sinsin
7	Arlon
8	Luxembourg
9	Namur
10	Anderlues
11	Storage
12	Peronnes
13	Blaregnies

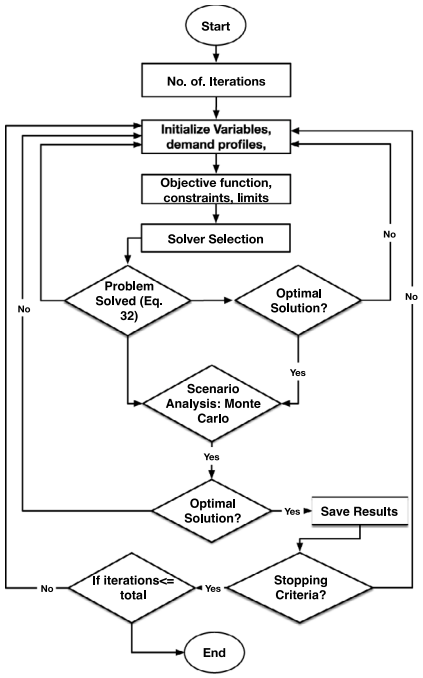

Fig. 2. Process flow of the proposed optimization mechanism.

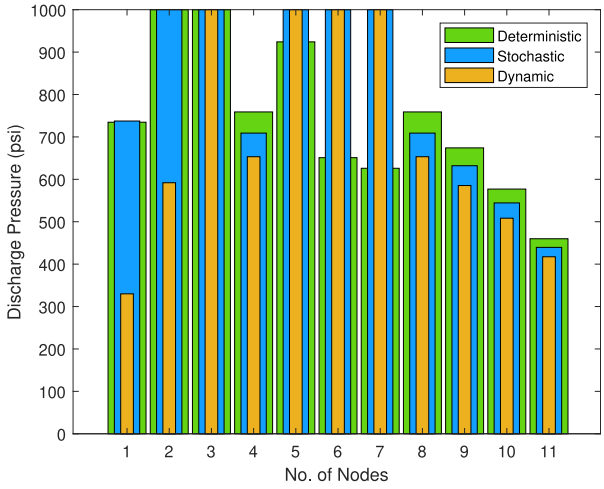

Fig. 3. A dynamic gas discharge pressure at the different nodes of Table 2.

varying demands by dynamically adjusting the number of compressors, allowing for more efficient resource allocation. This is in stark contrast to the deterministic and stochastic methods, which operate with fixed compressor settings and fail to account for real-time demand fluctuations. As a result, the deterministic and stochastic approaches show higher variability in discharge pressures across the nodes, whereas the dynamic approach maintains a more stable and optimized pressure distribution. This performance is achieved through the use of the CPLEX solver, which directly solves the Mixed-Integer Nonlinear Programming (MINLP) problem without requiring linearization, thereby allowing for more accurate and responsive compressor scheduling.

In Fig. 4, the comparison of gas flow, discharge, suction, and pressure drop at various nodes further highlights the advantages of the dynamic approach. Specifically, the dynamic scheduling algorithm results in a more balanced and optimized flow across the network. This is crucial in real-world applications where demand can change rapidly, and the system must adapt to maintain optimal flow and pressure conditions. The dynamic approach integrates real-time gas flow (MMCFD) considerations into the optimization, which ensures that each node operates under optimal conditions, thereby improving overall system efficiency. In contrast, both the deterministic and stochastic methods show greater pressure drops and less optimal flow profiles, indicating suboptimal resource allocation. The stochastic and dynamic algorithms (Fig. 4b,c) give a relatively balanced profile across nodes (8–11) due to the selection of diameter and length of the pipes (Table 3). Similarly, Fig. 4a gives a low flow rate across nodes (4–7), which is due to the selection of a constant diameter (18 inches) of the pipe. Moreover, the selection of length across node (4) seems non-optimal, which is unexpectedly increased in the deterministic approach, causing a pressure drop. The inclusion of gas flow in the objective function, unlike similar work where this was not accounted for, allows for a more comprehensive optimization of the network's operations. By addressing both the variability in discharge pressure (Fig. 3) and the overall system flow and pressure profiles (Fig. 4), the proposed approach demonstrates its ability to outperform traditional methods in terms of efficiency, resource allocation, and response to demand fluctuations. These enhancements make the dynamic approach particularly well-suited for real-time operational management in complex gas networks.

Fig. 5 shows the comparison of flow rates across each node. It reflects that the flow dynamically changes across each node depending on the supply–demand creation, lower and upper limits, and scheduling uncertainties. However, the overall operation is completed to fulfil the required objective. The figure also shows that the deterministic algorithm exhibits higher flow rates at nodes 8–10, while the stochastic and dynamic algorithms display more consistent profiles due to the dynamic behaviour of the control variables during the implementation and decision process.

Fig. 6 presents the pressure drop profiles at each compressor. The loss function is included in the objective function, which depends on the compressor types and specifications. The maximum pressure drop is observed at nodes 3, 5, and 7, where the deterministic technique outperforms the other techniques. However, the overall performance of the dynamic technique is better, primarily due to the mismatch between the dynamic pressure on the supply and demand sides. The pressure drop at the remaining nodes is reasonably lower, which can be attributed to the selection of valves, junctions, and compressors.

Fig. 7 displays the profiles of the suction pressure across each node along with the minimum and maximum limits. Initially, the suction pressure in the dynamic technique shows a continuously increasing trend, which leads to decreased costs compared to the other techniques. It is clear from Fig. 8 that the dynamic algorithm significantly reduces operating costs (59.98%), primarily due to the optimal selection of compressor stations (four stations in total). In contrast, the deterministic and stochastic algorithms show comparatively higher operating costs, as six to seven compressors are required in these approaches. Consequently, the compressor capital cost is also lower in the dynamic algorithm, highlighting its cost efficiency. However, it is important to note that the pipe capital cost in the dynamic algorithm is marginally higher (0.084%) than in the stochastic algorithm and (3.49%) more than in the deterministic approach. This increase stems from the selection of a slightly longer pipeline across node 3 (143 km). Despite this, the overall reduction in operating and compressor costs validates the superior performance of the dynamic algorithm in terms of cost optimization.

Table 3 shows the relationship between the diameter and length of the H_2 pipeline network across the given number of nodes. These results demonstrate the variation in length and diameter selection during the implementation process. The dynamic flow has impacted the optimal selection of the diameter. This variation is due to changes in H_2 flow pressure based on the demand profiles. Similarly, Table 4 presents

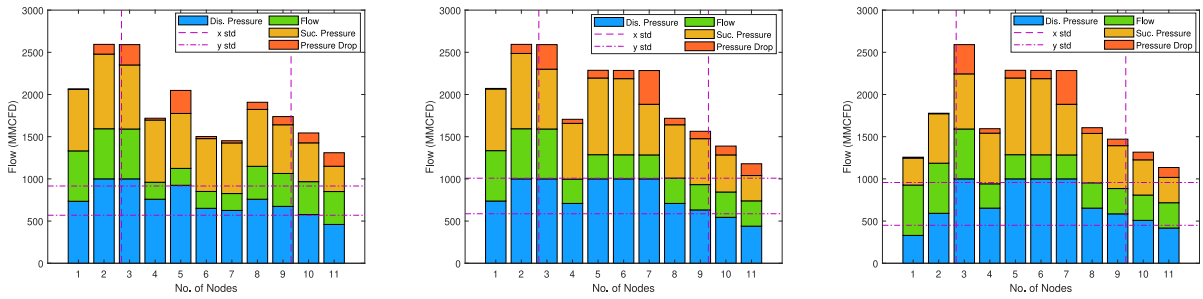

(a) Deterministic approach. (b) Stochastic approach. (c) Dynamic approach.

Fig. 4. A comparison of gas flow, discharge, suction, and drop in pressure at the different nodes of Table 2.

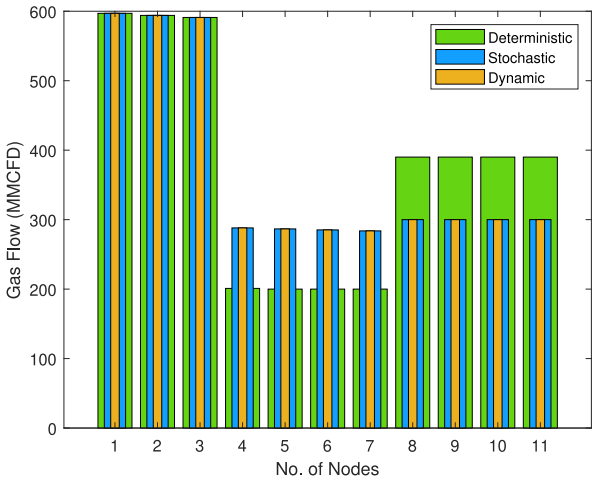

Fig. 5. Gas flow at the different nodes of Table 2.

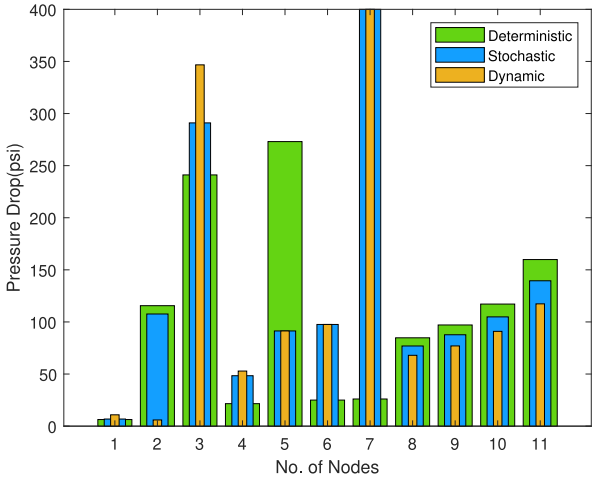

Fig. 6. Gas pressure drop at the different nodes of Table 2.

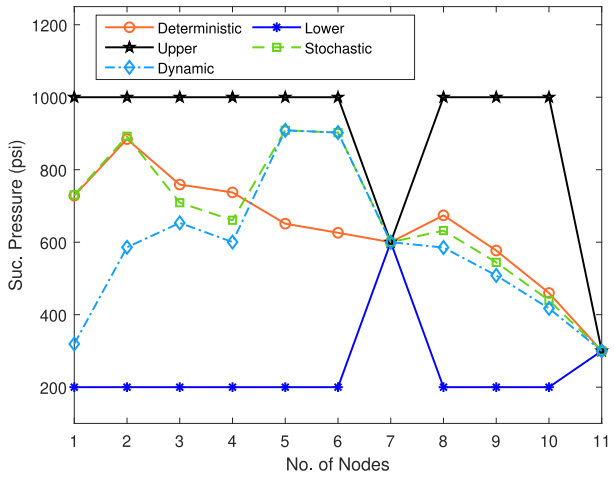

Fig. 7. Gas pressure at the different nodes with lower and upper limits.

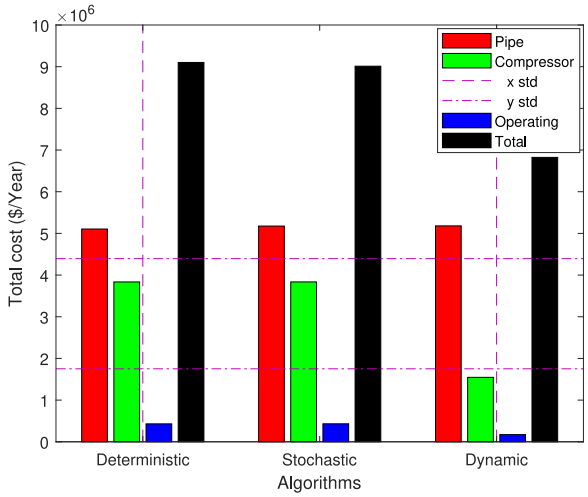

Fig. 8. Total capital cost of the H_2 transmission network to meet the demand.

the compressor ratios and workloads, comparing scenarios with fixed pressure using the Eq. (25) (ratio-1 and work-1) and dynamic demand (ratio-2 and work-2). Table 5 extends this comparison by including a probabilistic approach with storage units, showing three different settings: fixed pressure without storage (ratio-1, work-1), integration of storage units (ratio-2, work-2), and both storage unit and dynamic flow rate (ratio-3, work-3). It is also worth mentioning that Table 4 shows results for only four compressors, whereas Table 5 includes results for six and seven compressors. This increased number of compressors helps to reduce the extra pressure on individual compressors through optimal pressure allocation across all compressors. Otherwise, selecting a smaller number of compressors may lead to excessive pressure drops.

A performance comparison of the three methodologies — stochastic, dynamic, and deterministic — is shown in Table 6. This analysis evaluates the impact of each method on the objective function, identifying the optimal values achieved by each approach. The dynamic

Table 3
Relationship between the diameter and length of the gas pipeline network.

	Nodes	1	2	3	4	5	6	7	8	9	10	11	12	13
Deterministic	Diameter	34.20	31.91	31.91	18.0	18.0	18.0	18.0	18.0	18.0	18.0	33.71	18.0	18.0
	Length	3.0	49.21	96.78	3.0	40.400	3.0	3.0	3.0	3.0	3.0	3.0	3.0	3.0
Probabilistic	Diameter	33.71	31.67	31.67	18.0	18.0	18.0	18.0	18.0	18.0	18.0	33.71	18.0	18.0
	Length	3.0	53.04	92.95	3.0	40.400	3.0	3.0	3.0	3.0	3.0	3.0	3.0	3.0
Deterministic with Storage	Diameter	34.20	31.61	31.61	18.0	18.0	18.0	18.0	16.76	16.76	16.76	33.71	16.76	16.76
	Length	3.0	38.97	107.02	3.0	16.53	13.70	16.16	3.0	3.0	3.0	3.0	3.0	3.0
Probabilistic with Storage	Diameter	33.71	31.39	31.39	18.0	18.0	18.0	18.0	16.82	16.82	16.82	33.71	16.82	16.82
	Length	3.0	42.11	103.88	3.0	7.97	8.57	29.85	3.0	3.0	3.0	3.0	3.0	3.0
Dynamic	Diameter	36.00	36.00	32.25	18.0	18.0	18.0	18.0	17.47	17.47	17.47	33.71	17.47	17.47
	Length	3.00	3.00	143.00	3.0	7.92	8.57	29.85	3.0	3.0	3.0	3.0	3.0	3.0

Table 4
Optimal selection of the compressors and comparison of work done based on ratio (Eq. (25)), Dynamic approach.

Sr. No	Compressor	Ratio-1	Work-1	Ratio-2	Work-2
1	C_1	1.469	9288.83	1.475	9384.46
2	C_2	1.373	7566.75	1.369	7488.469
3	C_3	1.131	2866.32	1.150	3274.98
4	C_5	1.253	1799.70	1.253	1799.70

Table 5
Optimal selection of the compressors and comparison of work done based on ratio (Eq. (25)), Probabilistic and deterministic approaches.

Sr. No	Compressor	Ratio-1	Work-1	Ratio-2	Work-2	Ratio-3	Work-3
1	C_1	1.469	9288.83	1.475	9384.46	2.00	17 214.88
2	C_2	1.373	7566.75	1.369	7488.469	1.85	15 160.67
3	C_3	1.104	2312.02	1.121	2654.71	1.70	12 949.58
5	C_5	1.500	4679.86	1.514	4818.90	1.66	5981.40
6	C_6	1.248	2502.46	1.101	1075.90	1.101	1075.90
7	C_7	–	–	1.108	1148.27	1.108	1148.27

method achieved the highest objective value, surpassing the stochastic and deterministic approaches by 6.94% and 5.34%, respectively. The stochastic technique yielded the best average solution, surpassing the dynamic and deterministic methods by 8.58% and 13.70%. Since, the simulations were conducted across 100 scenarios for 100 iterations using Monte Carlo simulation, considering variations in pipe & operating costs as well as suction & discharge pressures with ±18.75% deviation. Notably, the total number of iterations required to complete the simulations was consistent across all methods, though execution time and iterations increased with the total number of scenarios. In addition, the optimality criteria are also validated via a convergence test. Regarding cost reduction, the proposed dynamic approach excels in cost reduction due to its adaptability to fluctuating demand and operational conditions. It optimizes compressor selection and scheduling, integrates storage facilities for efficient gas management, and effectively addresses uncertainties in cost, suction, and discharge pressures. This holistic strategy enables global optimization, leading to lower operating costs and enhanced system efficiency, ultimately resulting in significant overall cost savings.

7. Conclusions and future work

In this study, we introduced a novel MINLP approach with CPLEX employing branch-and-cut and branch-and-bound algorithms to address the complex hydrogen gas network problem in the Belgian network. Utilizing a graph theory-based framework, our model optimizes the primal MINLP problem with a strong focus on cost reduction. We reduce computational delays by leveraging discrete and continuous optimizers such as DICOPT with CPLEX or CONOPT solvers through integer variable fixing. Unlike conventional methods that rely heavily on branch-and-bound for NLP, our strategy enables dynamic hydrogen demand management, incorporating storage facilities without excessive dependence on historical datasets and control variables. The proposed model demonstrates adaptability by incorporating deterministic, stochastic, and dynamic techniques, each suitable for different scenarios. The deterministic approach offers simplicity and computational efficiency but lacks flexibility when dealing with uncertainties in demand. The stochastic method accounts for uncertainty but is computationally more expensive. In contrast, the dynamic technique, which is the core of our work, adapts in real-time to fluctuating demand, offering superior performance in terms of resource allocation and computational efficiency. Our results demonstrate that the dynamic approach significantly reduces the number of iterations (56 iterations) compared to deterministic (92 iterations) and stochastic (77 iterations) methods, achieving a 25.02% cost reduction while maintaining robustness.

The advantages of the dynamic approach, including real-time adaptability and superior computational performance, make it particularly well-suited for large-scale, complex hydrogen network transmission planning. However, deterministic and stochastic methods remain valuable in specific application scenarios, such as when system uncertainties are minimal or known in advance. Our approach has been validated through real-world simulations, effectively addressing the challenges associated with hydrogen network optimization and planning in large-scale systems. Building on these findings, our future work aims to expand the hydrogen network to include electricity or water distribution networks, adopting a holistic energy system approach. This aims to advance sustainable and efficient hydrogen networks, transforming clean energy technology and its practical application. To achieve this, several key areas will be addressed:

- Model Complexity: addressing the high complexity and computational demands of the current model, which may limit scalability and applicability to other networks.
- Integration Challenges: exploring the integration of hydrogen networks with electricity and water systems, and managing their interdependencies and impact on performance.
- Real-Time Data Integration: combining real-time and historical data for improved prediction and long-term forecasting, while addressing data synchronization and reliability issues.
- Demand-Side Management: enhancing demand forecasting to optimize network planning and utilization, considering factors like consumer behaviour, demand variation, environmental influences, technological advancements, and policy changes.

Table 6
Performance comparison of different algorithms.

Algorithm	Exe. time (s)	Best sol.	Avg. sol.	Std. dev.	Sol.	Iter.
Deterministic	8.937	6796965.745	7019837.219	121375.297	Optimal	112
Stochastic	8.406	7005929.375	6452271.910	306275.029	Optimal	104
Dynamic	7.860	6452271.910	7005929.375	307817.986	Optimal	104

CRediT authorship contribution statement

M.B. Rasheed: Visualization, Writing – original draft, Software, Data curation, Validation, Formal analysis, Writing – review & editing, Methodology, Conceptualization. **Daniel Rodriguez:** Writing – review & editing, Software, Methodology, Visualization, Project administration, Data curation, Supervision, Writing – original draft, Resources, Funding acquisition, Validation, Investigation, Conceptualization. **Maria D. R-Moreno:** Investigation, Visualization, Software, Writing – original draft, Supervision, Project administration, Formal analysis, Writing – review & editing, Validation, Resources, Methodology, Conceptualization.

Declaration of competing interest

The authors declare that they have no known competing financial interests or personal relationships that could have appeared to influence the work reported in this paper.

Acknowledgements

This project has received funding from the European Union Horizon 2020 research and innovation program under the Marie Skłodowska-Curie grant agreement No 754382, GOT ENERGY TALENT. In addition, Maria D. R-Moreno is supported by JCLM project SBPLY/24/180225/000143, and Daniel acknowledges that this publication is part of the project PID2021-125645OB-I00 (PARCHE), funded by MCIN/AEI/10.13039/501100011033/FEDER, EU.

Data availability

No data was used for the research described in the article.

References

[1] C. Ruocco, V. Palma, A. Ricca, Kinetics of oxidative steam reforming of ethanol over bimetallic catalysts supported on CeO2–SiO2: a comparative study, Top. Catal. 62 (5) (2019) 467–478.
[2] Z. Abdin, A. Zafaranloo, A. Rafiee, W. Mérida, W. Lipiński, Khalilpour K.R., Hydrogen as an energy vector, Renew. Sustain. Energy Rev. 120 (2020) 109620.
[3] I. Dincer, Green methods for hydrogen production, Int. J. Hydrog. Energy 37 (2) (2012) 1954–1971.
[4] N.L. Reddy, V.N. Rao, M. Vijayakumar, R. Santhosh, S. Anandan, M. Karthik, M.V. Shankar, K.R. Reddy, N.P. Shetti, M.N. Nadagouda, T.M. Aminabhavi, A review on frontiers in plasmonic nano-photocatalysts for hydrogen production, Int. J. Hydrog. Energy 44 (21) (2019) 10453–10472.
[5] C.V. Reddy, K.R. Reddy, N.P. Shetti, J. Shim, T.M. Aminabhavi, D.D. Dionysiou, Hetero-nanostructured metal oxide-based hybrid photocatalysts for enhanced photoelectrochemical water splitting–a review, Int. J. Hydrog. Energy 45 (36) (2020) 18331–18347.
[6] S. Sharma, S. Basu, N.P. Shetti, T.M. Aminabhavi, Waste-to-energy nexus for circular economy and environmental protection: recent trends in hydrogen energy, Sci. Total. Environ. 713 (2020) 136633.
[7] K.V. Karthik, C. Reddy, K.R. Reddy, R. Ravishankar, G. Sanjeev, R.V. Kulkarni, N.P. Shetti, A.V. Raghu, Barium titanate nanostructures for photocatalytic hydrogen generation and photodegradation of chemical pollutants, J. Mater. Sci.: Mater. Electron. 30 (23) (2019) 20646–20653.
[8] S. Singla, S. Sharma, S. Basu, N.P. Shetti, K.R. Reddy, Graphene/graphitic carbon nitride-based ternary nanohybrids: Synthesis methods, properties, and applications for photocatalytic hydrogen production, FlatChem 24 (2020) 100200.
[9] U. Sikander, S. Sufian, M.A. Salam, A review of hydrotalcite based catalysts for hydrogen production systems, Int. J. Hydrog. Energy 42 (31) (2017) 19851–19868.
[10] Y.K. Salkuyeh, B.A. Saville, H.L. MacLean, Techno-economic analysis and life cycle assessment of hydrogen production from different biomass gasification processes, Int. J. Hydrog. Energy 43 (20) (2018) 9514–9528.
[11] C.C. Elam, C.E. Padró, G. Sandrock, A. Luzzi, P. Lindblad, E.F. Hagen, Realizing the hydrogen future: the international energy agency's efforts to advance hydrogen energy technologies, Int. J. Hydrog. Energy 28 (6) (2003) 601–607.
[12] G. Duman, K. Akarsu, A. Yilmazer, T.K. Gundogdu, N. Azbar, J. Yanik, Sustainable hydrogen production options from food wastes, Int. J. Hydrog. Energy 43 (23) (2018) 10595–10604.
[13] T.L. LeValley, A.R. Richard, M. Fan, The progress in water gas shift and steam reforming hydrogen production technologies–A review, Int. J. Hydrog. Energy 39 (30) (2014) 16983–17000.
[14] O.L. de Weck, D. Roos, C.L. Magee, C.M. Vest, Life-cycle properties of engineering systems: the ilities.
[15] M.H. Amini, O. Karabasoglu, Optimal operation of interdependent power systems and electrified transportation networks, Energies 11 (1) (2018) 196.
[16] S. Xie, Y. Xu, X. Zheng, On dynamic network equilibrium of a coupled power and transportation network, IEEE Trans. Smart Grid 13 (2) (2021) 1398–1411.
[17] A.M. Farid, Electrified transportation system performance: Conventional versus online electric vehicles, in: The on-Line Electric Vehicle, Springer, Cham, 2017, pp. 279–313.
[18] A.S. Stillwell, C.W. King, M.E. Webber, I.J. Duncan, A. Hardberger, The energy-water nexus in Texas, Ecol. Soc. 16 (1) (2011).
[19] K.S. Ayyagari, S. Wang, N. Gatsis, A.F. Taha, M. Giacomoni, Energy-efficient optimal water flow considering pump efficiency, in: 2021 IEEE Madrid PowerTech, IEEE, 2021, pp. 1–6.
[20] D.J. Thompson, A.M. Farid, A reference architecture for the American multi-modal energy system, 2020, arXiv preprint arXiv:2012.14486.
[21] E. Crawley, B. Cameron, D. Selva, System Architecture: Strategy and Product Development for Complex Systems, Prentice Hall Press, 2015.
[22] W.C. Schoonenberg, A.M. Farid, Evaluating engineering systems interventions, in: Handbook of Engineering Systems Design, Springer International Publishing, Cham, 2021, pp. 1–25.
[23] D. De Wolf, Y. Smeers, The gas transmission problem solved by an extension of the simplex algorithm, Manag. Sci. 46 (11) (2000) 1454–1465.
[24] Hasan Mehrjerdi, Reza Hemmati, Wind-hydrogen storage in distribution network expansion planning considering investment deferral and uncertainty, Sustain. Energy Technol. Assess. 39 (2020) 100687.
[25] W. Liu, C. Jiang, G. Geng, A tensor-based framework for multi-layer energy networks: Application to hydrogen systems, Appl. Energy 269 (2020) 114983.
[26] S.E. Hosseini, A.M. Andwari, M.A. Wahid, Multi-layer optimization of hydrogen transport systems: A graph theory approach, Renew. Sustain. Energy Rev. 136 (2021) 110450.
[27] T. Ishimatsu, O.L. de Weck, J.A. Hoffman, Y. Ohkami, R. Shishko, Generalized multicommodity network flow model for the earth–moon–mars logistics system, J. Spacecr. Rocket. 53 (1) (2016) 25–38.
[28] T. Ding, W. Jia, M. Shahidehpour, A convex energy-like function for reliable gas flow solutions in gas transmission systems, IEEE Trans. Power Syst. 36 (5) (2021) 4876–4879, http://dx.doi.org/10.1109/TPWRS.2021.3090262.
[29] Q. Chen, T. Zhang, M. Qadrdan, Assessing techno-economic and environmental impacts of gas compressor fleet as a source of flexibility to the power system, IEEE Trans. Energy Mark. Policy Regul. http://dx.doi.org/10.1109/TEMPR.2023.3276308.
[30] K. Ben Safta, J.M. Kisse, Hydrogen pipeline network design: An optimization-based planning method considering the existing natural gas network, in: PESS PELSS 2022, Power and Energy Student Summit, Kassel, Germany, 2022, pp. 1–6.
[31] S.K.K. Hari, K. Sundar, S. Srinivasan, A. Zlotnik, R. Bent, Operation of natural gas pipeline networks with storage under transient flow conditions, IEEE Trans. Control Syst. Technol. 30 (2) (2022) 667–679, http://dx.doi.org/10.1109/TCST.2021.3071316.
[32] Adarsh Kumar Arya, Optimal operation of a multi-distribution natural gas pipeline grid: an ant colony approach, J. Pet. Explor. Prod. Technol. 11 (10) (2021) 3859–3878.
[33] C. Shui, D. Zhou, Z. Wu, W. Yu, L. Zhang, T. Xing, C. Wang, Z. Du, Short-term operation optimization for natural gas pipeline considering line-pack: A perspective of optimal transport, Gas Sci. Eng. (2023) 205075.
[34] A.M. Farid, Reconfigurability Measurement in Automated Manufacturing Systems Doctoral dissertation, University of Cambridge.
[35] A.M. Farid, D.C. McFarlane, Production degrees of freedom as manufacturing system reconfiguration potential measures, Proc. Inst. Mech. Eng. Part B: J. Eng. Manuf. 222 (10) (2008) 1301–1314.

[36] A.M. Farid, Facilitating ease of system reconfiguration through measures of manufacturing modularity, Proc. Inst. Mech. Eng. Part B: J. Eng. Manuf. 222 (10) (2008) 1275–1288.
[37] A.M. Farid, D.J. Thompson, W. Schoonenberg, A tensor-based formulation of hetero-functional graph theory, Sci. Rep. 12 (1) (2022) 1–22.
[38] A.K. Arya, S. Honwad, Multiobjective optimization of a gas pipeline network: an ant colony approach, J. Pet. Explor. Prod. Technol. 8 (2018) 1389–1400.
[39] Compressible gas flow pressure drop, flow rate, pipe diameter, 2022, https://www.pipeflowcalculations.com/pipe-valve-fitting-flow/compressible-gas-flow.xhtml, (Accessed 12 July 2022).
[40] Weymouth, panhandle a and b equations for compressible gas flow, 2022, https://www.lmnoeng.com/Flow/weymouth.php, (Accessed 12 July 2022).
[41] S. Moran, An Applied Guide To Process and Plant Design, Elsevier, 2019.
[42] H. Zhang, Y. Liang, X. Zhou, X. Yan, C. Qian, Q. Liao, Sensitivity analysis and optimal operation control for large-scale waterflooding pipeline network of oilfield, J. Pet. Sci. Eng. 154 (2017) 38–48.
[43] B. Coulbeck, Dynamic simulation of water distribution systems, Math. Comput. Simulation 22 (3) (1980) 222–230.
[44] A. Santhosh, A.M. Farid, K. Youcef-Toumi, Optimal network flow for the supply side of the energy-water nexus, in: IEEE International Workshop on Inteligent Energy Systems, IWIES, Vienna, 2013, pp. 155–160, http://dx.doi.org/10.1109/IWIES.2013.6698578.
[45] U.Y. Shamir, C.D. Howard, Water distribution systems analysis, J. Hydraul. Div. 94 (1) 219–234.
[46] Chapter 1 hydraulics and head loss equations basic equations, 1984, pp. 1–20, [Online]. Available: http://www.sciencedirect.com/science/article/pii/S0167564808701497.
[47] T. Haktanr, M. Ardcloglu, Numerical modelling of Darcy–weisbach friction factor and branching pipes problem, Adv. Eng. Softw. 35 (12) (2004) 773–779, [Online]. Available: http://www.sciencedirect.com/science/article/pii/S0965997804001358.
[48] European Hydrogen Backbone (EHB), A vision towards a European hydrogen backbone, 2022, [Online]. Available at: https://www.ehb.eu/vision-2022.
[49] Gas for Climate, The European hydrogen backbone: How a dedicated hydrogen infrastructure can be created, 2020, Available at: https://www.gasforclimate2050.eu.
[50] H. Wang, L. Durand, P. Crespo, Challenges of hydrogen transmission in repurposed gas pipelines: A technical review, Int. J. Hydrog. Energy 46 (58) (2021) 29847–29857.
[51] Cadent, HyNet north west: Unlocking a low carbon future, 2021, Available at: https://hynet.co.uk/.
[52] HyDeploy, Project Overview: Hydrogen blending into the gas grid. Available: https://hydeploy.co.uk.